Full perturbation solution for the flow in a rotating torus

A. Chupin and R. Stepanov
Institute of Continuous Media Mechanics, Korolyov 1, Perm 614013, Russia
(Received 25 February 2008; published 27 May 2008)

We present a perturbation solution for a pressure-driven fluid flow in a rotating toroidal channel. The analysis shows the difference between the solutions of full and simplified equations studied earlier. The result is found to be reliable for *low* Reynolds number (Re), as was the case for a previously studied solution for high Re. The convergence conditions are defined for the whole range of governing parameters. The viscous flow exhibits some interesting features in flow pattern and hydrodynamic characteristics.

DOI: 10.1103/PhysRevE.77.057301 PACS number(s): 47.60.Dx

I. INTRODUCTION

Fluid flow in a general curved pipe is known not to be one-dimensional since the pioneering work of Dean [1]. A secondary flow develops when a fluid is driven by pressure gradient in a toroidal channel. In practice, this occurs in many applications: channels in industry, blood vessels in physiology, transport pipe systems, coolant pipe systems, and others. In a considerable number of studies, there has been a strong motivation for finding a solution for flows in a curved channel.

A stationary solution of the Navier-Stokes equation in a curved pipe was first analyzed by the perturbation method [1]. An analytical solution was obtained for a *simplified* equation valid at a low value of the Dean number $\mathrm{De}=\mathrm{Re}\,\kappa^{1/2}$. This solution was compared with the results of direct numerical simulation for the wide range of governing parameters [2]. The case of a rotating channel was first studied in [3]. Later many authors considered this problem using different approaches. Pressure drop, heat, and mass transfers were studied in detail (for review, see, e.g., [2]). Non-Newtonian fluid flow in a curved pipe shows a specific behavior for different rheologic cases (see, e.g., [4] and references therein). Magnetic field induction was experimentally studied in conductive fluid flow in toroidal channel [5].

In this Brief Report, we derive a perturbation analytical solution of the *full* equations taking into account all curvature effects. It is shown that the well known solution [1] corresponds to the case $\mathrm{Re}\gg 1$. In the general case, the solution cannot be parametrized by the Dean number only. The suggested solution properly describes the case of low Reynolds number (Re) and asymptotically approaches the known solution at high Re. For high viscosity of the fluid, the inertial terms in the Navier-Stokes equation are relatively unimportant and the flow pattern is determined by a balance of viscous forces and the pressure gradients in the fluid. Such flows, called creeping flows, are of nearly the same importance in practice as the inertial flows (with $\mathrm{Re}\gg 1$).

II. MATHEMATICAL MODEL

A curved pipe is considered as a toroidal channel with the outer radius r_c and radius of the inner circular section R. We use a coordinate system $\{\rho,\varphi,\zeta\}$, where ρ and φ are polar coordinates in the cross section and ζ is the linear coordinate along the channel (see Fig. 1). The torus revolves around its main axis with a constant angular velocity Ω ($\Omega>0$ means corotation with respect to the direction of the flow driven by a pressure gradient). The flow of an incompressible fluid in the rotating channel is governed by the equations

$$\frac{\partial \mathbf{v}}{\partial t}+\mathbf{v}\cdot\nabla\mathbf{v}=-2\boldsymbol{\Omega}\times\mathbf{v}-\frac{\nabla p}{\rho_0}+\nu\Delta\mathbf{v},$$

$$\nabla\cdot\mathbf{v}=\mathbf{0}, \tag{1}$$

where $\mathbf{v}$ is the velocity in the rotating frame of reference, ρ_0 is the fluid density, and ν is the kinematic viscosity.

After introducing the vorticity $\boldsymbol{\omega}=\nabla\times\mathbf{v}$, pressure can be eliminated. The resulting *Helmholtz equation* is written as

$$\frac{\partial \boldsymbol{\omega}}{\partial t}+(\mathbf{v}\cdot\nabla)\boldsymbol{\omega}-(\boldsymbol{\omega}\cdot\nabla)\mathbf{v}=-2\,\nabla\times(\boldsymbol{\Omega}\times\mathbf{v})+\nu\Delta\boldsymbol{\omega}. \tag{2}$$

Assuming that the flow is stationary and ζ-independent, Eqs. (1) and (2) can be reduced to the equations for two scalar functions: stream velocity v_ζ and stream function ψ, which is defined in such way that

$$\{v_\rho,v_\varphi,0\}=\nabla\times(\psi\hat{\boldsymbol{\zeta}}). \tag{3}$$

The no-slip boundary conditions

$$v_\zeta|_{\rho=1}=\psi|_{\rho=1}=\left.\frac{\partial\psi}{\partial\rho}\right|_{\rho=1}=0 \tag{4}$$

together with the regularity condition at the centerline must be satisfied. Following arguments in [6], we assume the pres-

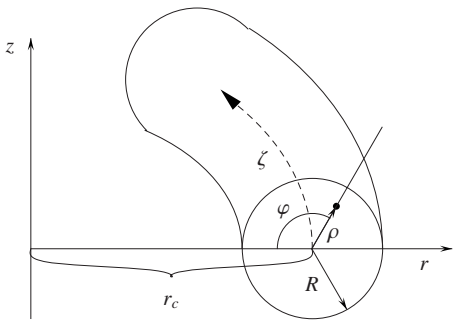

FIG. 1. The coordinate system in the toroidal channel.

sure to be a linear function of ζ. Therefore, the pressure gradient is constant along the channel.

Choosing V as the characteristic velocity, the inner radius R as the characteristic length, and Q as the characteristic pressure gradient, we introduce dimensionless variables $\rho^*=\rho/R$, $\zeta^*=\zeta/R$, $v_\zeta^*=v_\zeta/V$, $\psi^*=\psi/(VR)$, and $p^*=pR/Q$. The following governing dimensionless parameters will be used: curvature ratio $\kappa=R/r_c$, Reynolds number $\mathrm{Re}=(VR)/\nu$, dimensionless angular velocity $F=(\Omega r_c)/V$, and pressure gradient parameter $G=(QR^2)/(\rho_0\nu V)$, which is a ratio of the viscous and pressure forces. $r=(\kappa^{-1}-\rho\cos\varphi)$ is the dimensionless distance from the torus axis.

Thus, the following set of equations describes the problem (the superscript " *" is omitted everywhere below):

$$(D_\varphi\psi D_r v_\zeta - D_r\psi D_\varphi v_\zeta) = 2\kappa F\left(\frac{\cos\varphi}{\rho}\frac{\partial\psi}{\partial\varphi}+\sin\varphi\frac{\partial\psi}{\partial\rho}\right) + \frac{G}{r\kappa\,\mathrm{Re}}+\frac{1}{\mathrm{Re}}\mathcal{L}v_\zeta, \tag{5}$$

$$D_r v_\zeta \hat{D}_\varphi v_\zeta - \hat{D}_r v_\zeta D_\varphi v_\zeta + D_r\psi\hat{D}_\varphi\mathcal{L}\psi - \hat{D}_r\mathcal{L}\psi D_\varphi\psi = 2\kappa F\left(\frac{\cos\varphi}{\rho}\frac{\partial v_\zeta}{\partial\varphi}+\sin\varphi\frac{\partial v_\zeta}{\partial\rho}\right)-\frac{1}{\mathrm{Re}}\mathcal{L}^2\psi, \tag{6}$$

while Eq. (3) in these coordinates leads to the expression for the stream function,

$$v_\rho = D_\varphi\psi = \frac{\psi\sin\varphi}{\kappa^{-1}-\rho\cos\varphi}+\frac{1}{\rho}\frac{\partial\psi}{\partial\varphi},$$

$$v_\varphi = -D_r\psi = \frac{\psi\cos\varphi}{\kappa^{-1}-\rho\cos\varphi}-\frac{\partial\psi}{\partial\rho}. \tag{7}$$

The remaining differential operators are

$$\hat{D}_r=\frac{\partial}{\partial\rho}+\frac{\cos\varphi}{r},\quad \hat{D}_\varphi=\frac{1}{\rho}\frac{\partial}{\partial\varphi}-\frac{\sin\varphi}{r}, \tag{8}$$

$$\Delta_{\mathrm{cyl}}=\frac{\partial^2}{\partial\rho^2}+\frac{1}{\rho}\frac{\partial}{\partial\rho}+\frac{1}{\rho^2}\frac{\partial^2}{\partial\varphi^2}, \tag{9}$$

$$\mathcal{L}=\Delta_{\mathrm{cyl}}-\frac{\cos\varphi}{r}\frac{\partial}{\partial\rho}-\frac{1}{r^2}+\frac{\sin\varphi}{\rho r}\frac{\partial}{\partial\varphi}. \tag{10}$$

The effect of curvature can be obtained after significant simplification of the governing Eqs. (5) and (6). The idea of Dean [1] was to renormalize the stream function by a factor of Re and combine factors Re $\kappa^{1/2}$ into the so-called Dean number. The approximation $\kappa\ll 1$ is applied after that. Terms with curvature ratio remain only in the first two advective terms and the Coriolis force term in Eq. (6). The limit $\kappa\ll 1$ at fixed value De corresponds to the limit $\mathrm{Re}\gg 1$. A perturbation solution of these *simplified* equations was reconsidered and compared with the results of direct numerical simulations in [2]. We solve Eqs. (5) and (6) in general. This means that the viscous term corresponding to the toroidal Laplacian operator $\mathcal{L}$ (10) is not replaced by a cylindrical one (9). The term corresponding to the Coriolis force in Eq. (5) remains. All curvature ratio contributions are kept in the advective terms and pressure gradient.

III. PERTURBATION SOLUTION

Solution of Eqs. (5) and (6) can be expanded in power series in a small parameter κ,

$$v_\zeta = v^{(0)}(\rho,\varphi)+\kappa v^{(1)}(\rho,\varphi)+\kappa^2 v^{(2)}(\rho,\varphi)+\cdots, \tag{11}$$

$$\psi = \psi^{(0)}(\rho,\varphi)+\kappa\psi^{(1)}(\rho,\varphi)+\kappa^2\psi^{(2)}(\rho,\varphi)+\cdots. \tag{12}$$

Expanding all operators (7)–(10) in the same series, we can write the zero-order approximation of Eqs. (5) and (6) as

$$J(v^{(0)},\psi^{(0)})=\frac{G}{\mathrm{Re}}+\frac{1}{\mathrm{Re}}\Delta_{\mathrm{cyl}}v^{(0)},$$

$$J(\Delta_{\mathrm{cyl}}\psi^{(0)},\psi^{(0)})=\frac{1}{\mathrm{Re}}\Delta_{\mathrm{cyl}}^2\psi^{(0)}, \tag{13}$$

where $J(A,B)$ is the Jacobian of the functions A and B with respect to ρ and φ,

$$J(A,B)=\frac{1}{\rho}\left(\frac{\partial A}{\partial\rho}\frac{\partial B}{\partial\varphi}-\frac{\partial B}{\partial\rho}\frac{\partial A}{\partial\varphi}\right). \tag{14}$$

This gives a solution corresponding to cylindrical geometry, namely to the Poiseuille flow

$$v^{(0)}=\frac{G}{4}(1-\rho^2),\quad \psi^{(0)}=0. \tag{15}$$

The first-order approximation leads to the system

$$J(v^{(1)},\psi^{(0)})+J(v^{(0)},\psi^{(1)})+\psi^{(0)}v^{(0)}\frac{\partial}{\partial z}\ln\frac{v^{(0)}}{\psi^{(0)}} = \frac{G}{\mathrm{Re}}\rho\cos\varphi-\frac{1}{\mathrm{Re}}\frac{\partial v^{(0)}}{\partial r}+\frac{1}{\mathrm{Re}}\Delta_{\mathrm{cyl}}v^{(1)}+2F\frac{\partial\psi^{(0)}}{\partial z}, \tag{16}$$

$$\frac{\Delta_{\mathrm{cyl}}^2\psi^{(1)}}{\mathrm{Re}} = J(\Delta_{\mathrm{cyl}}\psi^{(0)},\psi^{(1)})+J(\Delta_{\mathrm{cyl}}\psi^{(1)},\psi^{(0)}) + 2(F+v^{(0)})\frac{\partial v^{(0)}}{\partial z}-\frac{2}{\mathrm{Re}}\frac{\partial}{\partial r}\Delta_{\mathrm{cyl}}\psi^{(0)}+J\left(\frac{\partial\psi^{(0)}}{\partial r},\psi^{(0)}\right) + \frac{\partial(\psi^{(0)}\Delta_{\mathrm{cyl}}\psi^{(0)})}{\partial z} \tag{17}$$

and its solution gives the first-order correction,

$$v^{(1)}=\frac{3G\cos\varphi}{16}\rho(1-\rho^2)+\frac{G^3\,\mathrm{Re}^2\cos\varphi}{737280}\rho(1-\rho^2)(\rho^6-9\rho^4+21\rho^2-19)-\frac{G^2F\,\mathrm{Re}^2\cos\varphi}{18432}\rho(1-\rho^2)(\rho^4-3\rho^2+3), \tag{18}$$

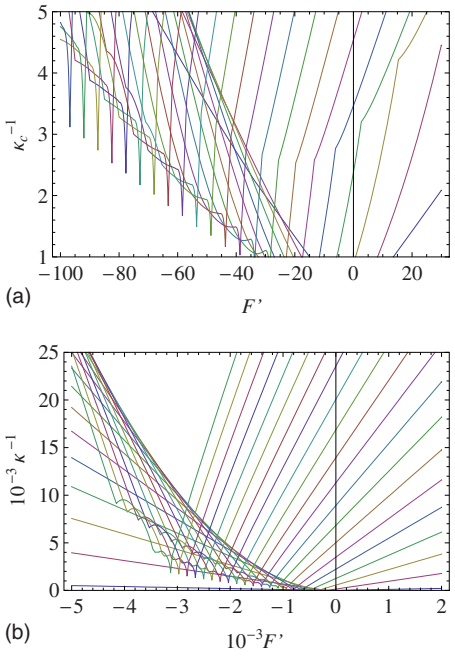

FIG. 2. (Color online) The dependence of convergence radius on F' for different values of G' (a) from 5 to 705 and (b) from 5 to 21 000.

$$\psi^{(1)} = \frac{G^2 \,\mathrm{Re} \sin\varphi}{4608}\rho(\rho^2-4)(\rho^2-1)^2 - \frac{GF\,\mathrm{Re}\sin\varphi}{192}\rho(\rho^2-1)^2. \tag{19}$$

This solution is different from the solution obtained by [2] (we denote the latter by superscript "c"). The first-order solution has an additional term,

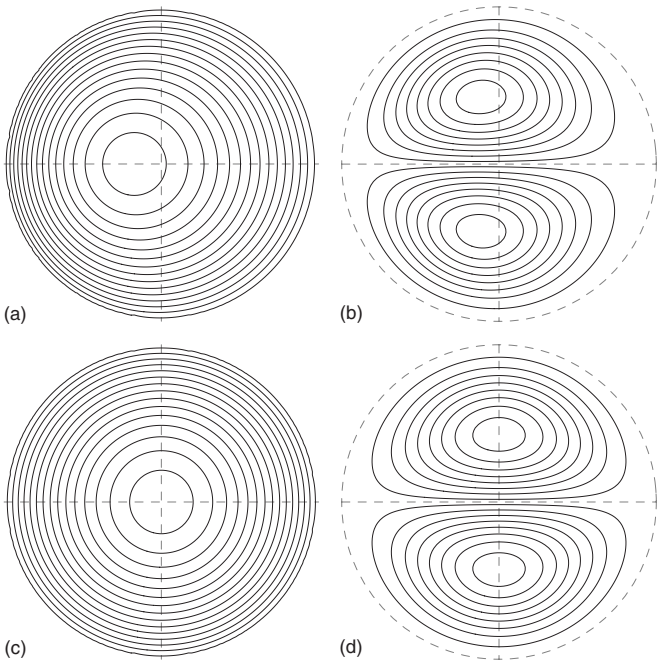

FIG. 3. $\kappa=0.5$, Re$=1$, $F=0$. Comparison of solutions. (a) v_ζ, (b) $v_\zeta^{(c)}$, (c) ψ, (d) $\psi^{(c)}$.

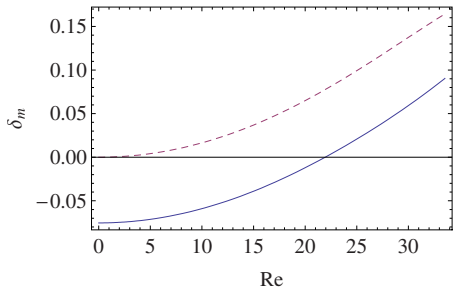

FIG. 4. (Color online) Horizontal shift δ_m of the stream velocity maximum vs Re at $\kappa=0.1$. Dashed line stands for the solution $v_\zeta^{(c)}$.

$$v_\zeta - v_\zeta^{(c)} = \kappa\frac{3G\cos\varphi}{16}\rho(1-\rho^2) + O(\kappa^2). \tag{20}$$

$\psi^{(1)}$ has no difference from that in [2]. The corrections of the second-order approximation $v^{(2)}$ and $\psi^{(2)}$ can be derived in a similar way. For the stream function, we find

$$\psi - \psi^{(c)} = -\kappa^2\frac{\rho^2(1-\rho^2)^2\sin 2\varphi}{92160}[150G\,\mathrm{Re}\,F + G^2\,\mathrm{Re}(56 - 17\rho^2)] + O(\kappa^3). \tag{21}$$

We note that κ and Re cannot be combined (for instance, in the Dean number) for parametrization of the present perturbation solution; both should be treated as independent parameters.

IV. CONVERGENCE

It is clear that the perturbation solution is valid, i.e., that the series converges, only at specific values of the governing parameters Re, F, G, and κ. The conditions on the governing parameters have been defined in order to satisfy the uniform convergence of the maximum value for each order of approximation.

All terms in the expressions for $v^{(i)}$ and $\psi^{(i)}$ have the form $(G\,\mathrm{Re})^j(F\,\mathrm{Re})^k/\mathrm{Re}$. So, for convergence analysis we use for convenience the following values: $G'=G\,\mathrm{Re}$ and $F'=F\,\mathrm{Re}$, which are the only factors that influence the convergence. The maximal powers of G' and F' included in $v^{(i)}$ grow as $2i+1$ and i accordingly. However, these powers can be reached only in different terms such as G'^{2i+1} and $G'^{i+1}F'^{i}/\mathrm{Re}$. So the radius of convergence should be $O(G'^{-2}+G'^{-1}F'^{-1})$. We estimate the radius of convergence κ_c with the following technique. A supposition of uniform convergence necessarily implies a monotonic decrease of $v^{(i)}$ majorants in Eq. (11). In order to know this, we evaluate terms up to fifth order, find the global maxima in the circle $\rho\leqslant 1$, and calculate the largest κ, for which the maxima do not increase.

Thus we obtain κ_c as a function of G' and F' (see Fig. 2), which is rather complex but displays some nice asymptotics. For $|F'|\gg 1$, we have obtained a dependence of the following kind: $a+b|F'-c|$. As curve fitting has shown, the coefficients a, b, and c are linear functions of $G'\gg 1$.

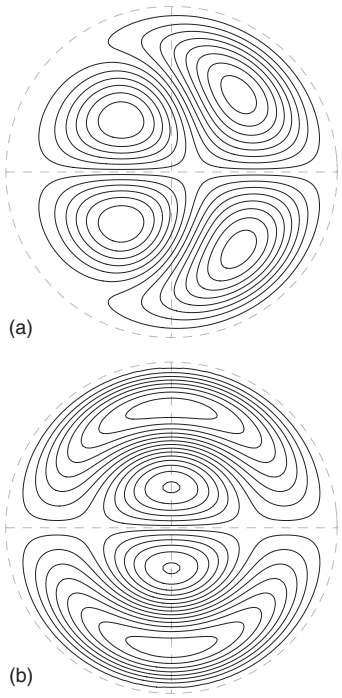

FIG. 5. $\kappa=0.5$, Re$=1$, $F=-0.63$. Comparison of solutions. (a) ψ, (b) $\psi^{(c)}$.

V. RESULTS

The solution was analyzed in detail in the earlier studies. There the attention was centered on the case of large Re. Our finding deals with the case of small Re when the viscous term is comparable to or larger than the convective one. This difference arises when new terms (20) and (21) in the solution (18) and (19) dominate, i.e., when Re is small.

One can see in Figs. 3(a) and 3(b) for the case $F=0$ and small Reynolds number that the solution $v_\xi^{(c)}$ is almost axisymmetric but the new solution v_ζ has nonaxisymmetric contribution (20). As a result of this, the stream velocity maximum is moved inwards. There is a similar difference between stream functions [see Figs. 3(c) and 3(d)]. This horizontal shift δ_m is produced by pressure and viscous forces, which are described by the first and the second terms on the right-hand side of Eq. (16). The centrifugal force starts to play a role when Re gets large. The inertia effect [nonlinear terms in Eqs. (16) and (17)] causes a shift of the stream velocity maximum outwards. The dependence δ_m(Re) is shown in Fig. 4. The offset between the two curves results from the simplifications used in [2], which are described in the last paragraph in Sec. II.

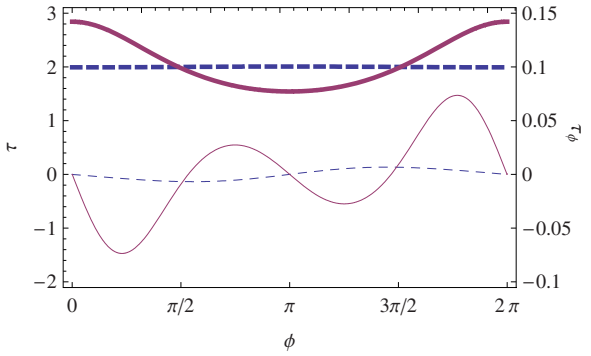

FIG. 6. (Color online) Axial shear stress τ (bold lines, tick labels at left) and azimuthal shear stress τ_φ (thin lines, tick labels at right) dependencies on angle. Dashed lines correspond to the solution in [2]. $\kappa=0.4$, Re$=10$, $F=-0.49$.

When the torus rotates ($F\neq 0$), the Coriolis force gives rise to additional vortices in the cross section. In the counter-rotating case, such a vortex can act against the centrifugal vortex. This produces a four-vortex picture (see Fig. 5). Again we see that the flow pattern is different for a low Reynolds number. The vortex corresponding to the Coriolis force arises at the boundary while $\psi^{(c)}$ starts to grow in the center.

Axial shear-stress along the channel $\tau=-\frac{\partial v_\xi}{\partial \rho}|_{\rho=1}$ differs from that presented in [2]. The first-order residual is $3/16G\kappa(3\rho^2-1)\cos\varphi$. It does not change the pressure drop but produces a strong variation (about 40%) of friction at the boundary (see Fig. 6, thick curves). There is a similar difference in the azimuthal shear stress $\tau_\varphi=-\frac{\partial v_\varphi}{\partial \rho}|_{\rho=1}$. The second-order residual is

$$\tau_\varphi-\tau_\varphi^c=\frac{G\,\mathrm{Re}(13G-25)\kappa^2\sin 2\varphi}{3840}. \tag{22}$$

This work shows that solution of the *full* governing equations reveals some specific features for flow in a toroidal channel: a shift of the maximum of the stream velocity toward the inner axis, the appearance of a second pair of vortices at the internal boundary, and an additional φ dependence of stresses. These are prominent at low values of the Reynolds number. The solution for a given curvature ratio κ asymptotically approaches the known solution [2] at high Re.

ACKNOWLEDGMENTS

This work was supported by RFBR-Ural Grant No. 06-01-00234 and the Russian Federation President Grant No. MK-4338.2007.1.

[1] W. R. Dean, Philos. Mag. **7**, 208 (1927).
[2] J. Zhang, N. Li, and B. Zhang, Phys. Rev. E **67**, 056303 (2003).
[3] H. Ito and T. Motai, Rep. Inst. High Speed Mech. (1974), p. 33.
[4] Y. Chen, H. Chen, J. Zhang, and B. Zhang, Phys. Fluids **18**, 3103 (2006).
[5] R. Stepanov, R. Volk, S. Denisov, P. Frick, V. Noskov, and J.-F. Pinton, Phys. Rev. E **73**, 046310 (2006).
[6] D. J. McConalogue and R. S. Srivastava, Proc. R. Soc. London, Ser. A **307**, 37 (1968).